JOURNAL OF CATALYSIS 148, 697–708 (1994)

Mechanistic Importance of Intermediate N_2O + CO Reaction in Overall NO + CO Reaction System

II. Further Analysis and Experimental Observations

Byong K. Cho

Physical Chemistry Department, NAO Research and Development Center, General Motors Corporation, Warren, Michigan 48090-9055

Received June 7, 1993; revised April 25, 1994

In an earlier kinetic analysis we predicted the mechanistic importance of the formation of N_2O and its subsequent reaction with CO in the overall NO + CO reaction system. This work has confirmed the previous theoretical findings through steady-state and transient pulse experiments using Rh catalysts supported on alumina, ceria, and modified ceria. Results have revealed that, in agreement with the theoretical analysis, the observed suppression of the product selectivity to N_2O during the NO + CO reaction at high temperatures is due to the fast N_2O + CO reaction following the formation of N_2O. Detailed analysis of the existing kinetic data in the literature indicates that the sticking coefficient of N_2O under typical reaction conditions is extremely small ($\sim 2 \times 10^{-6}$) and thus the rate-limiting step of the isolated N_2O + CO reaction is the adsorption of N_2O onto the catalyst surface. Both the overall reaction pathways and the lightoff behavior of the NO + CO reaction system are discussed in light of these experimental findings. This study also serves to elucidate the nature of the low-temperature N_2 desorption step (i.e., $NO_a + N_a \rightarrow N_2 + O_a + S$) previously reported in the literature.

INTRODUCTION

Due largely to its importance for automotive exhaust emission control, the mechanism of NO + CO reaction on noble metal catalysts, especially on Rh catalysts, has been extensively investigated since the early 1980s (e.g., 1—12). However, the participation of N_2O + CO reaction as an intermediate reaction step during the overall NO + CO reaction has been recognized only recently. For example, Hecker and Bell (4, 5) observed the formation of N_2O during the NO + CO reaction over Rh/SiO_2 in the low-temperature regime, but further reaction of N_2O with CO was found to be negligible. Recently Cho *et al.* (9) observed not only the formation of N_2O but the further reaction of N_2O with CO over Rh/Al_2O_3, which was later confirmed by McCabe and Wong (13).

In view of the above historical developments in our understanding of the interactions of NO and CO with Rh surfaces, a comprehensive mechanistic model of the NO + CO reaction has been proposed as (9, 12)

$$NO + S \leftrightharpoons NO_a \quad [1]$$

$$CO + S \leftrightharpoons CO_a \quad [2]$$

$$NO_a + S \rightarrow N_a + O_a \quad [3]$$

$$NO_a + N_a \rightarrow N_2O_a + S \quad [4]$$

$$N_2O_a \leftrightharpoons N_2O + S \quad [5]$$

$$N_2O_a \rightarrow N_2 + O_a \quad [6]$$

$$N_a + N_a \rightarrow N_2 + 2S \quad [7]$$

$$CO_a + O_a \rightarrow CO_2 + 2S, \quad [8]$$

where the subscript "a" denotes adsorbed state. Note that the surface reaction mechanisms previously reported in the literature for the NO + CO reaction are special cases of the elementary surface processes shown above. For example, Hecker and Bell (4) used

$$NO_a + N_a \rightarrow N_2O + 2S \quad [9]$$

in place of Eqs. [4] and [5], and

$$NO_a + N_a \rightarrow N_2 + O_a + S \quad [10]$$

in place of Eqs. [4] and [6]. On the other hand, Oh *et al.* (8) adopted only Eq. [10] in place of Eqs. [4]–[6]. In light of our comprehensive mechanistic model, the model used by Hecker and Bell (4) can be considered as a special case when both the desorption rate and dissociation rate of N_2O_a are assumed to be very fast compared with the rate of N_2O_a formation, whereas the model employed by Oh *et al.* (8) can be treated as another special case when

0021-9517/94 $6.00

the dissociation rate of N_2O_a is very fast compared with the rate of N_2O_a formation and/or the desorption rate is very slow compared with the rate of N_2O_a formation and dissociation.

For convenience in our discussion, the elementary surface processes shown in Eqs. [1]–[8] can be combined to the following overall reaction scheme for the NO + CO reaction over supported Rh catalysts:

$$NO + CO \rightarrow \tfrac{1}{2}N_2 + CO_2 \quad [11]$$

$$2\,NO + CO \rightarrow N_2O + CO_2 \quad [12]$$

$$N_2O + CO \rightarrow N_2 + CO_2. \quad [13]$$

The first reaction pathway (Eq. [11]) represents direct reduction of NO to N_2 in a single step, without forming the N_2O (and N_2O_a) intermediate; it involves elementary surface processes [1]–[3], [7], and [8]. Note that the gas-phase intermediate (N_2O) and the surface intermediate (N_2O_a) cannot be treated separately due to the exchange process occurring between them through adsorption and desorption. Reaction [12] represents partial reduction of NO to N_2O via elementary surface processes [1]–[5] along with [8], while reaction [13] represents further reduction of N_2O to N_2 via elementary surface processes [5], [6], and [8]. Thus, reactions [12] and [13] constitute a two-step reaction pathway involving the N_2O intermediate, as opposed to the one-step reaction pathway of Eq. [11] involving N_2 desorption via N_a–N_a recombination. It is important to recognize here that the elementary surface processes underlying in the two-step reaction pathway (i.e., Eqs. [12] and [13]) embrace the low-temperature N_2 desorption pathway proposed previously in the literature (1, 4, 7, 8).

We wish to point out that the importance of the two-step reaction pathway has not been fully appreciated in the literature of the past decade, and that there are two main reasons behind this situation. One reason is that in general the formation of N_2O has not been observed during the NO + CO reaction on Rh surfaces (7, 8), or in some instances where N_2O was detected, a small amount of N_2O was observed to form only over a narrow temperature range (9, 11). The other reason is that the rate of the isolated N_2O + CO reaction (Eq. [13] by itself) has been reported to be very slow compared with that of the NO + CO reaction (Eq. [11]) (4, 13, 14). Under the circumstances, one would be tempted to assume that the two-step reaction pathway involving Eqs. [12] and [13] is not important in the overall NO reduction process.

Recently, however, it has been shown experimentally that the N_2O formation is significant in a low-temperature regime, where the NO + CO reaction lights off (9, 13). Furthermore, it has also been shown theoretically that the rate of the N_2O + CO reaction as an *intermediate* reaction step in the overall NO + CO reaction system can be as fast as or even faster than the NO + CO reaction, even though the N_2O + CO reaction as an *isolated* reaction system is very slow (12). These observations suggest that the two-step reaction pathway involving the formation of N_2O and its subsequent reaction with CO can make an important contribution to the overall kinetics of the NO + CO reaction over supported Rh catalysts. In this work, we present experimental evidence to confirm the mechanistic importance of the two-step reaction pathway, a feature that has previously been predicted by the kinetic analysis (12). This study also serves to elucidate the nature of the low-temperature N_2 desorption step (Eq. [10]) previously proposed in the literature.

EXPERIMENTAL

Having shown that the intermediate N_2O + CO reaction can be as fast as the overall NO + CO reaction in our previous kinetic analysis (12), we now demonstrate the mechanistic importance of the N_2O formation as well as the rate enhancement of the N_2O + CO reaction using both steady-state and transient experimental schemes as follows.

Effect of Space Velocity on N_2O Formation during NO + CO Reaction

Previously, N_2O has been observed during the NO + CO reaction only at low temperatures around the reaction lightoff temperature, with no significant amount of N_2O observed at temperatures above 300°C (9, 13). In view of the very slow rate of the isolated N_2O + CO reaction compared with that of the NO + CO reaction, this observation of no N_2O at high temperatures above 300°C might be attributed to the absence of N_2O formation, possibly leading to the conclusion that at high temperatures above 300°C the NO + CO reaction proceeds via the reaction pathway [11] without forming the intermediate N_2O.

Having realized that the rate of the intermediate N_2O + CO reaction can be as fast as or even faster than the NO + CO reaction (12), it seems reasonable to propose another plausible explanation for this absence of N_2O at high temperatures; the N_2O formed as an intermediate during the NO + CO reaction may have reacted with CO so fast that N_2O could not be detected under experimental conditions of interest. To examine this latter possibility, we carried out steady-state NO + CO reaction experiments under stoichiometric conditions at different space velocities—approximately 10^5, 10^6, and 10^7 h^{-1}. Since the reaction products CO_2 and N_2O have the same mass number of 44, ^{13}CO isotope was used in place of CO so that $^{13}CO_2$ (mass number = 45) could easily be separated from N_2O by a mass spectrometer. The purity of ^{13}C atoms in ^{13}CO was 99%. The logic behind this

TABLE 1

Reactor Experiments at Different Space Velocities

	Regular reactor	Microreactor	Ultramicroreactor
Reactor tube size[a] (cm O.D.)	0.32	0.16	0.16
Catalyst[b]	Rh/Al_2O_3	Rh/Al_2O_3	Rh/Al_2O_3
Catalyst bed depth (cm)	1	0.5	0.05
Sample weight (mg)	22	1.6	0.22
Gas flowrate (STP) (cm^3/min)	50	50	50
Space velocity (STP) (h^{-1})	8.6×10^4	1.5×10^6	1.1×10^7
Temperature (°C)	200–500	200–500	200–500
Pressure (kPa)	101.3	101.3	101.3

[a] All three reactors were made of stainless steel tube.
[b] Detailed description of the Rh/Al_2O_3 sample can be found in the literature (11).

experimental scheme is that, if N_2O formation is indeed an intermediate step during the NO + CO reaction, N_2O should be detected in significant quantities even at high temperatures above 300°C when the space velocity is increased to compensate for the increased temperature. In varying the space velocity, we reduced the reactor volume while keeping the total flow rate constant; a microreactor was used for the space velocity of 10^6 h^{-1}, and an ultramicroreactor was used for the space velocity of 10^7 h^{-1}. Reactor temperature was measured at the inlet of the reactor bed. Detailed experimental conditions are listed in Table 1, and additional routine procedures such as catalyst pretreatment were the same as those used previously (11).

Results of reactor experiments at the space velocity of 8.6×10^4 h^{-1} are shown in Fig. 1, where the total conversion of NO can be compared with the conversion of NO to N_2O. Note in Fig. 1 that N_2O formation is most pronounced at the reaction lightoff temperature, and that it is not observed at high temperatures above 300°C. When we increased the space velocity of the experiments from 8.6×10^4 h^{-1} to 1.2×10^6 h^{-1} by reducing the reactor volume while keeping the gas flow rate constant, we obtained the results shown in Fig. 2, which clearly demonstrate that N_2O forms at high temperatures well above 300°C. Comparing the N_2O concentration at 310°C in Fig. 1 with that in Fig. 2, we can conclude that the absence of N_2O in the gas phase in Fig. 1 is not because N_2O does not form at that temperature, but because the N_2O produced quickly disappears due to its reaction with CO on the catalytic surface. (One may argue that, even in the absence of the intermediate N_2O + CO reaction, the selectivity of N_2O formation could decline at high temperatures if the mass transfer rate of N_2O from the catalyst surface to the bulk gas stream could not keep up with the rate of N_2O formation on the surface. However, detailed analysis indicates that this hypothesis can be ruled out, because the mass transfer rate is much faster than the maximum possible N_2O formation rate even at those high temperatures, as shown in Appendix B.) When the space velocity of the experiments was further increased to 1.1×10^7 h^{-1}, N_2O formation was observed even at higher temperatures, as shown in Fig. 3. Comparing Figs. 1–3, we note that the peak of N_2O formation decreases with increasing space velocity. Though a detailed discussion on this behavior is beyond the scope of this paper, a simple explanation can be made in terms of differences in activation energies as follows. The activation energy for N_2O dissociation (18 kcal/mol (14)) is much larger than that for N_2O desorption (5–6 kcal/mol (13, 14)), so the rate of N_2O dissociation increases more quickly with temperature than the rate of N_2O desorption. Thus, the de-

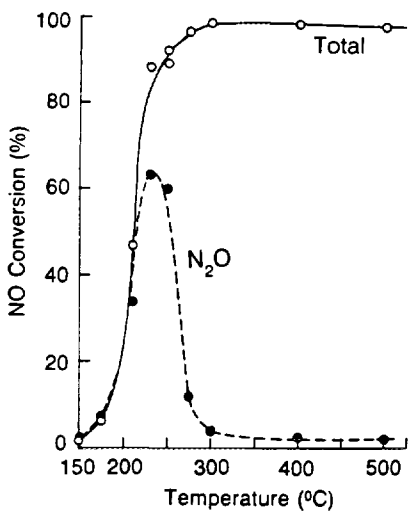

FIG. 1. Comparison of total NO conversion with N_2O formation during the NO + CO reaction over Rh/Al_2O_3 (space velocity = 8.6×10^4/h, (○) total NO conversion, (●) NO conversion to N_2O).

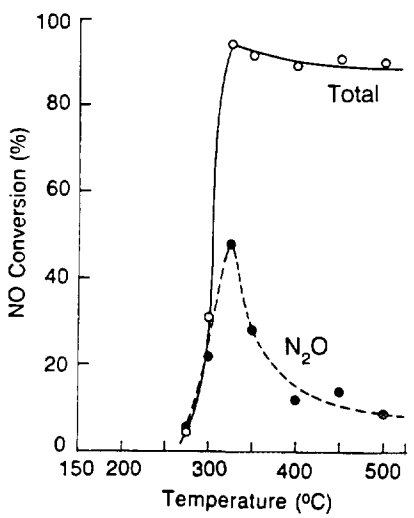

FIG. 2. Comparison of total NO conversion with N_2O formation during the NO + CO reaction over Rh/Al_2O_3 (space velocity = 1.5×10^6/h, (○) total NO conversions, (●) NO conversion to N_2O).

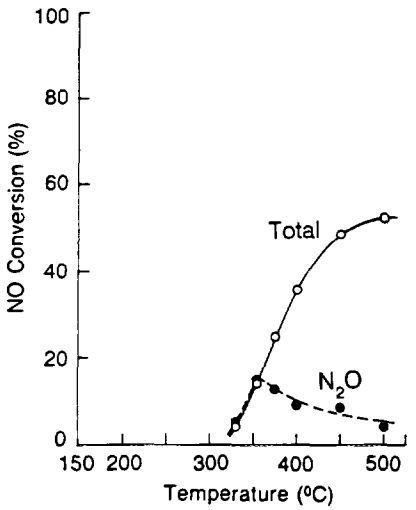

FIG. 3. Comparison of total NO conversion with N_2O formation during the NO + CO reaction over Rh/Al_2O_3 (space velocity = 1.1×10^7/h, (○) total NO conversion, (●) NO conversion to N_2O).

sorption probability of N_2O_a decreases relative to its dissociation probability, as the increase in space velocity shifts the reactor operating regime toward higher temperatures.

With the above findings in mind, we now turn to Fig. 1 and focus on the fact that, at high temperatures above 300°C, all the NO conversion results in N_2. In view of Figs. 2 and 3, this conversion of NO exclusively to N_2 cannot be explained simply on the basis of the single-step reaction pathway, Eq. [11]. Furthermore, the single-step reaction pathway is not consistent with the result of the kinetic analysis (12), where the desorption of N_2 via N_a–N_a recombination is shown to be negligible below 500°C during the NO + CO reaction over Rh catalysts. Hence, both the earlier theoretical analysis (12) and experimental data in this work indicate that the two-step reaction pathway via Eqs. [12] and [13] makes an important contribution in the reduction of NO by CO over a temperature range much wider than previously thought.

Transient Rate Enhancement of N_2O + CO Reaction during Cyclic Operation between NO + CO Reaction and N_2O + CO Reaction

In our previous kinetic analysis (12), we have shown that the rate of the N_2O + CO reaction as an intermediate reaction step in the overall NO + CO reaction system can be much faster than the rate of the N_2O + CO reaction as an isolated reaction. The rate enhancement was explained by the combined effect of increased surface concentration of N_2O and the decreased inhibition effect on the catalytic surface in the NO + CO system compared with those in the isolated N_2O + CO system. Of the two effects contributing to the rate enhancement, the decreased inhibition effect on the catalytic surface during the NO + CO reaction can be verified experimentally by using a cyclic operation between the N_2O + CO reaction and the NO + CO reaction. The rationale behind this experimental scheme is presented below.

To understand the transient catalytic activity of Rh/Al_2O_3 during the cyclic operation between the NO + CO and N_2O + CO reactions, it is useful to apply the concept of the inhibition function developed previously (12). This inhibition function (Δ), which quantifies the inhibiting effect of adsorbed species on the surface reaction rate, is defined as

$$\Delta = (\beta + r_2)(1 + \Gamma_{CO}) + (1 - r_2)\Gamma_{N_2O}, \qquad [14]$$

where

$$\Gamma_{CO} = K_{CO}C_{CO}, \qquad \Gamma_{N_2O} = \beta K_{N_2O}C_{N_2O}, \qquad [15]$$

$$\beta = k_{d,N_2O}/k_{d,CO}, \qquad r_2 = k_{N_2O}/k_{d,CO}, \qquad [16]$$

and the definitions of other notations are listed in Appendix A.

Now suppose we have a cyclic operating condition between the NO + CO reaction and the N_2O + CO reaction such as the one depicted in Fig. 4. In this cycling scheme, NO flow (denoted by the solid area) and N_2O flow (denoted by the dotted area) are alternately fed to the reactor in the presence of constant CO flow. The duty fraction of the NO half-cycle is kept the same as that of the N_2O half-cycle, resulting in a symmetric cycling scheme. In this way, both the NO + CO reaction and the N_2O + CO reaction can be kept at the stoichiometric point during the cycling experiments. At the transition point from the NO to the N_2O flow, the catalytic surface can be assumed to be equilibrated under the NO + CO reaction condition. Thus, the rate of the N_2O + CO reaction at this transition point ($\tilde{R}_i$) can be written as

$$\tilde{R}_i = \beta_o k_{N_2O} K_{N_2O} C_{N_2O}/\Delta_o, \qquad [17]$$

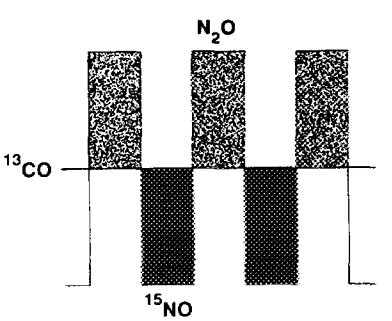

FIG. 4. The cycling scheme used for cyclic operation between the NO + CO reaction and the N_2O + CO reaction (cycling period = 20 s).

where β_0 and Δ_0 are the values of β and Δ under the overall NO + CO reaction condition (12). On the other hand, the steady-state rate of the N_2O + CO reaction (R_i) is

$$R_i = \beta_i k_{N_2O} K_{N_2O} C_{N_2O}/\Delta_i, \quad [18]$$

where β_i and Δ_i denote the values of β and Δ under the isolated N_2O + CO reaction condition (12). The rate enhancement factor at this transition point ($\tilde{\eta}$) can then be written as

$$\tilde{\eta} = \tilde{R}_i/R_i = (\beta_0/\beta_i)(\Delta_i/\Delta_0). \quad [19]$$

When a switch is made from the NO flow to the N_2O flow (Fig. 4), the inhibition function due to the surface coverage starts to change from Δ_0 to Δ_i in response to the change in the gas-phase environment, while the value of β starts to change from β_0 to β_i. This then suggests that the rate of the N_2O + CO reaction at this transition point must be enhanced by the multiple of the $(\beta_0\Delta_i)/(\beta_i\Delta_0)$ ratio (Eq. [19]) compared with its rate under the steady-state condition. Figure 5 shows the transient rate-enhancement factor ($\tilde{\eta}$) calculated for both $S_{N_2O} = 2 \times 10^{-3}$ and $S_{N_2O} = 2 \times 10^{-6}$ as a function of temperature. Clearly, $\tilde{\eta}$ is not sensitive to S_{N_2O} in this range of the S_{N_2O} values over the entire temperature range shown. (Here the transient rate-enhancement factor ($\tilde{\eta}$) should not be confused with the steady-state rate-enhancement factor (η) of the intermediate N_2O + CO reaction; η has been shown to be very sensitive to S_{N_2O} (12).) Figure 5 indicates that this type of cyclic operation can enhance the transient rate of the N_2O + CO reaction in the temperature range between 200 and 600°C, with a maximum enhancement expected to occur at around 240°C.

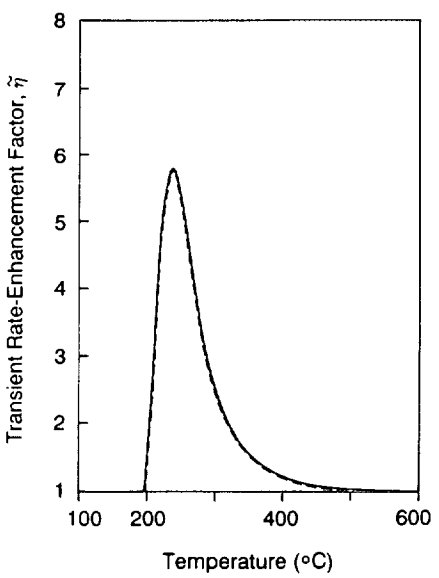

FIG. 5. Transient rate-enhancement factor ($\tilde{\eta}$) at the transition point from the NO + CO half-cycle to the N_2O + CO half-cycle during the cyclic operation as a function of temperature ((---)$S_{N_2O} = 2 \times 10^{-6}$; (—)$S_{N_2O} = 2 \times 10^{-3}$).

The possibility of rate enhancement of the N_2O + CO reaction due to the reduced inhibition function during the transient period of the (NO + CO)/(N_2O + CO) cyclic operation discussed above was verified experimentally in the cylcic operating experiment such as is shown in Fig. 4. Details of the cycling experiments are listed in Table 2. Note that ^{13}CO was used in place of CO to separate mass spectroscopically N_2O from $^{13}CO_2$, while ^{15}NO was used in place of NO to distinguish between N_2 derived from N_2O dissociation and $^{15}N_2$ derived from ^{15}NO dissociation. The purities of ^{13}C atoms in ^{13}CO, and ^{15}N atoms in ^{15}NO were both 99%. (For convenience, CO and NO will be used to denote ^{13}CO and ^{15}NO, respectively, unless clarity requires the use of the full notation.) For the purpose of comparison, we also carried out steady-state experiments for both the N_2O + CO and NO + CO reactions over Rh/Al_2O_3; at 275°C the steady-state conversion of N_2O during the N_2O + CO reaction was 8%, while that of NO during the NO + CO reaction was close to 100%, confirming that the steady-state rate of the isolated N_2O + CO reaction is indeed much slower than that of the NO + CO reaction.

Presented in Fig. 6 are reactor outlet concentrations measured during the symmetric cyclic operation between the NO + CO feed and the N_2O + CO feed over Rh/Al_2O_3 with a cycling period of 20 s at 275°C. The dotted lines in Figs. 6a and 6b represent the N_2O and NO signals, respectively, at a reactor temperature of 25°C, where the Rh/Al_2O_3 catalysts exhibited no measurable activity for both the N_2O + CO and NO + CO reactions. The reactor outlet concentrations of N_2O and NO at 275°C are also shown in Figs. 6a and 6b in solid lines. Thus, the areas between the dotted lines and the solid lines in Figs. 6a and 6b represent the conversions of N_2O and NO during

TABLE 2

Experimental Conditions for Cyclic Operation between NO + CO Reaction and N_2O + CO Reaction

Catalyst and reactor	Same as that used in the regular reactor listed in Table 1.
Space velocity (STP) (h^{-1})	8.4×10^4
Cycling mode	Symmetric cycling
Cycling period(s)	20
Feed concentration	^{15}NO = 400 ppm in He ^{13}CO = 400 ppm in He N_2O = 400 ppm in He
Temperature (°C)	275
Pressure (kPa)	101.3

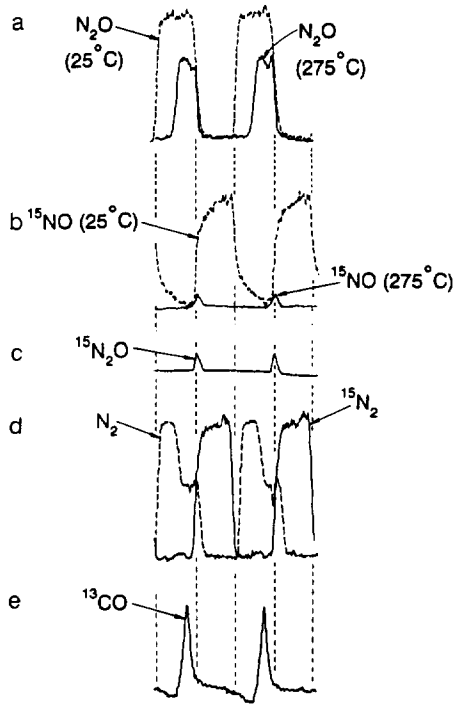

FIG. 6. Time variations of the reactor outlet concentrations during symmetric cycling operation between the NO + CO system and the N_2O + CO system (cycling period = 20 s; feed concentrations, $C_{CO} = C_{NO} = C_{N_2O} = 400$ ppm in He).

the N_2O + CO and NO + CO reactions at 275°C, respectively. It should be noted in Figs. 6a and 6b that the catalyst exhibits high activity for the N_2O + CO reaction as well as for the NO + CO reaction under the cyclic operating condition. The time-average conversions of NO and N_2O under the cycled operating conditions were 98 and 72%, respectively. Remember that the N_2O conversion during the steady-state N_2O + CO reaction was only 8%. At the end of the N_2O half-cycle (Fig. 6a), the N_2O conversion (~30%) remains much higher than the steady-state conversion level, indicating that a complete steady state has not yet been attained at the end of the N_2O half-cycle.

It is particularly remarkable to see that the N_2O conversion during the first 4 s of the N_2O half-cycle reaches 100% before the catalytic activity abruptly drops. The conversion of N_2O in Fig. 6a corresponds very closely to the production of N_2 shown in Fig. 6d as well as to the conversion of CO shown in Fig. 6e. As expected, the NO conversion during the NO half-cycle is close to 100% (Fig. 6b), which is consistent with both the production of $^{15}N_2$ shown in Fig. 6d and the conversion of CO shown in Fig. 6e. Although it is not clear why the CO concentration profile exhibits a sharp peak in Fig. 6e, we speculate that it may be due to the disappearance of CO from the gas phase via adsorption process (in parallel with the reaction process) during the transient period. It is also noteworthy that a small amount of $^{15}N_2O$ is produced during the early part of the ^{15}NO half-cycle (Fig. 6c).

Perhaps the most interesting and important finding in this dynamic experiment is that the N_2O + CO reaction proceeds very quickly immediately after the catalyst has been exposed to the NO + CO reaction environment, even though the steady-state N_2O + CO reaction is very slow. Surprising as it may appear, this is very consistent with the results of our earlier kinetic analysis (12); during the N_2O + CO reaction, the catalyst surface is predominantly covered by CO and thus the reaction rate is limited by the availability of N_2O on the surface (see Table 3). On the other hand, during the NO + CO reaction, the adsorbed CO no longer dominates the catalyst surface and there are more vacant sites available for adsorption and dissociation of N_2O than during the N_2O + CO reaction. This difference in surface coverages between the N_2O + CO reaction condition and the NO + CO reaction condition makes the ratio of the inhibition function (Δ_i/Δ_o) substantially greater than one, while making the β_o/β_i ratio smaller than one. For example, at 275°C the Δ_i/Δ_o and β_o/β_i ratios become about 16 and 0.23, respectively, resulting in the transient rate-enhancement factor of approximately 4 as shown in Fig. 5. This clearly indicates that the inhibition effect (Δ) due to the adsorbed species under the NO + CO reaction condition is much smaller than that under the N_2O + CO reaction condition. When the N_2O + CO feed is just introduced at the completion of the NO + CO half-cycle, the catalyst surface still retains the surface coverage corresponding to the NO + CO reaction condition while beginning to adjust to the N_2O + CO reaction condition. Because of the reduced inhibition effect on the surface due to the preceding NO + CO half-cycle, the rate of the N_2O + CO reaction at the start of the N_2O half-cycle can be much faster than that under the steady-state condition. The surface coverages calculated from the previous kinetic analysis are listed in Table 3. The abrupt decrease of the catalyst

TABLE 3

Comparison of Surface Coverages (T = 275°C)

Surface coverage	NO + CO system	N_2O + CO system
θ_{CO}	0.439	0.959
θ_{N_2O}	0.361×10^{-7}	0.638×10^{-10}
θ_v	0.154	0.041
θ_N	0.392	0.0
θ_{NO}	0.150	0.0

Note. (1) Kinetic parameters used in the calculation were those reported previously (12); (2) $C_{CO} = C_{NO} = 400$ ppm in He was used for the NO + CO system; (3) $C_{CO} = C_{N_2O} = 400$ ppm in He was used for the N_2O + CO system.

activity for the N_2O conversion in the middle of the N_2O half-cycle shown in Fig. 6a can also be attributed to the change of the surface coverages from those characteristic of the NO + CO environment to the N_2O + CO environment.

Effect of Catalyst Support on N_2O Formation during NO + CO Reaction

So far we have shown that N_2O formation and its subsequent reaction with CO are important intermediate steps in the NO + CO reaction over Rh/Al_2O_3. In view of the wide practice of using ceria as an additive in automotive three-way catalysts, it is useful to examine whether N_2O formation is also significant during the NO + CO reaction over Rh catalysts impregnated on different supports such as ceria (CeO_2) and modified ceria (CeO_2-a) (11). Thus, we have carried out a series of additional steady-state experiments using Rh/CeO_2 and Rh/CeO_2-a catalysts. Here CeO_2-a denotes an activated form of ceria obtained by chemical modification of ceria (11). Details of experimental conditions as well as the characteristics of the catalysts can be found elsewhere (11).

Presented in Figs. 7a and 7b are the total conversion of NO and the amount of N_2O formation, respectively, as a function of catalyst temperature during the steady-state NO + CO reaction over Rh/Al_2O_3, Rh/CeO_2, and Rh/CeO_2-a. (The amount of N_2O formation over Rh/CeO_2 is not presented in Fig. 7b for clarity, since it is very similar to that over Rh/CeO_2-a.) The differences in the lightoff temperature for NO conversion among these three catalysts shown in Fig. 7a can be explained by the difference in Rh dispersion among those catalysts (11). We note that the pattern of N_2O formation shown in Fig. 7b is the same for both Rh/Al_2O_3 and Rh/CeO_2-a. Also, comparison of Figs. 7a and 7b indicates that the onset of the NO + CO reaction is always accompanied by the formation of N_2O for these catalysts. Note in Fig. 7b that Rh/Al_2O_3 produces N_2O between 175 and 300°C, whereas Rh/CeO_2-a produces N_2O between 275 and 500°C. This is another example of N_2O formation at high temperatures, observed when the active Rh surface area is decreased. Interestingly, however, the N_2O peaks shown in Fig. 7b remains almost constant, even though the temperature of their occurrence is different. This behavior is different from what we observed in Figs. 1 and 2 for Rh/Al_2O_3, for which we do not have a clear explanation yet. These observations, together with our earlier observations under the cyclic operating conditions (9), suggest that N_2O formation is an intrinsic characteristic of the NO + CO reaction over dispersed Rh particles, irrespective of the type of support. This supports our earlier conclusion that N_2O formation is an important intermediate step during the NO + CO reaction over supported Rh catalysts.

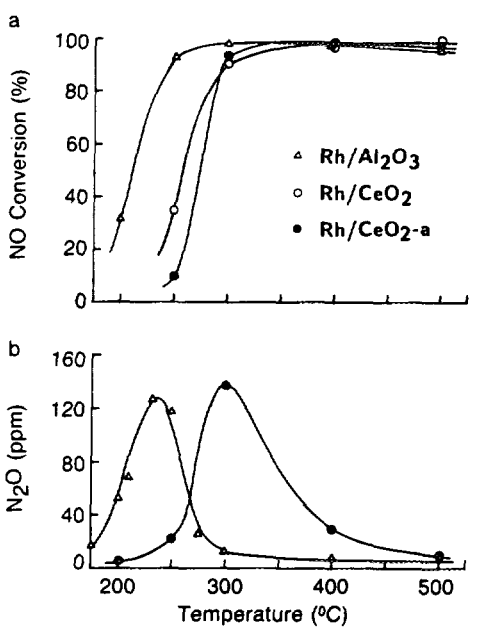

FIG. 7. Effect of catalyst support composition on N_2O formation during the NO + CO reaction (feed concentrations, $C_{NO} = C_{CO} = 800$ ppm in He).

ANALYSIS OF EXISTING KINETIC DATA FOR N_2O + CO REACTION

Theoretically, the mechanistic importance of the intermediate N_2O + CO reaction is directly related to its steady-state rate enhancement relative to the slow rate of the isolated N_2O + CO reaction; the intermediate N_2O + CO reaction becomes important only when the steady-state rate enhancement factor (η) is much larger than unity (12). On the other hand, the steady-state rate enhancement becomes significant only when the sticking coefficient of N_2O (S_{N_2O}) is much smaller than unity (12). In light of these previous findings, our experimental demonstration so far of the importance of the intermediate N_2O + CO reaction indicates that S_{N_2O} must be much smaller than unity. In the following, we confirm this by estimating the sticking coefficient of N_2O under reaction conditions, and identify the rate-limiting step (RLS) of the isolated N_2O + CO reaction.

Estimation of the Sticking Coefficient of N_2O under Reaction Conditions from Existing Kinetic Data

Since the sticking coefficient of N_2O over Rh/Al_2O_3 under reaction conditions is not available in the literature, we estimate it by applying the results of the previous kinetic analysis (12) to the existing steady-state kinetic data of the isolated N_2O + CO reaction reported by McCabe and Wong (13), as shown below.

The rate of the isolated N_2O + CO reaction (R_i) can be written as (12)

$$R_i = \frac{k_{N_2O}\Gamma_{N_2O}}{(\beta + r_2)(1 + \Gamma_{CO}) + (1 - r_2)\Gamma_{N_2O}}. \quad [20]$$

The inverse of the reaction rate is equivalent to the overall time constant (τ_0) for the isolated N_2O + CO reaction, and it can be expressed as a sum of two different time constants (τ_r and τ_∞)

$$\tau_0 = 1/R_i = \tau_r + \tau_\infty, \quad [21]$$

by defining τ_r and τ_∞ in such a way that

$$\tau_r = \frac{1 + K_{CO}C_{CO}}{C_{N_2O}}\left(\frac{1}{K_{N_2O}k_{N_2O}} + \frac{1}{k_{a,N_2O}}\right), \quad [22]$$

$$\tau_\infty = \frac{1}{K_{N_2O}} - \frac{1}{k_{d,CO}}. \quad [23]$$

It is useful to note in Eq. [22] that τ_r becomes very small when the N_2O concentration (C_{N_2O}) is much larger than the CO concentration (C_{CO}). (Note that $C_{N_2O} \gg C_{CO}$ corresponds to an extremely lean condition.) This means that the contribution of τ_r to the overall time constant of the N_2O + CO reaction becomes negligible under extremely lean (i.e., oxidizing) conditions, which means that τ_∞ in Eq. [21] physically represents the time constant for the N_2O + CO reaction under extremely lean conditions. In fact, under extremely lean conditions, the self-poisoning effect due to the accumulation of oxygen produced from the decomposition of N_2O reduces the decomposition rate of N_2O to a negligible level as observed by McCabe and Wong (13). Under typical steady-state operating conditions of the N_2O + CO reaction (where a significant amount of CO is present in the feed), however, the oxygen concentration on the catalyst surface is generally low because the oxygen produced by N_2O decomposition would be rapidly consumed by reaction with CO (13). The self-poisoning effect of the accumulated oxygen can therefore be neglected under the normal reaction conditions. Thus, τ_r in Eq. [21] represents the time constant under reaction conditions not too far from the stoichiometric condition.

The above discussion indicates that τ_r can be used for kinetic analysis of the isolated N_2O + CO reaction system under normal reaction conditions not far from the stoichiometric condition. Insertion of τ_r (Eq. [22]) into Eq. [21] reveals that a plot of $1/R_i$ vs $(1 + K_{CO}C_{CO})/C_{N_2O}$ should yield a straight line with a slope of $\{1/K_{N_2O}k_{N_2O} + 1/k_{a,N_2O}\}$, from which k_{a,N_2O} can be estimated if $K_{N_2O}k_{N_2O}$ is known. (In fact, the value of $K_{N_2O}k_{N_2O}$ was reported by McCabe and Wong (13).) The sticking coefficient of N_2O can then be determined from k_{a,N_2O}. Figure 8 shows a plot of $1/R_i$ vs $(1 + K_{CO}C_{CO})/C_{N_2O}$, where R_i, C_{CO}, and C_{N_2O} were obtained from the steady-state kinetic data and experimental conditions of McCabe and Wong (13) for the N_2O + CO reaction at 583 K. Since K_{CO} is a function of θ_{CO}, which is in turn a function of K_{CO}, the value of K_{CO} was calculated by a trial-and-error method using the parameter values shown previously (12). The stoichiometric number (S) shown in Fig. 8 is defined as the ratio of N_2O concentration to CO concentration. That is,

$$S = C_{N_2O}/C_{CO}.$$

Thus, the stoichiometric condition corresponds to S = 1, while the lean and rich conditions are represented by $S > 1$ and $S < 1$, respectively.

Interestingly, the straight line in Fig. 8 changes its slope at a slightly lean condition (i.e., $S \simeq 1.5$). The sticking coefficient of N_2O determined from the slope of the straight line A on the rich side along with the known value of $k_{N_2O}K_{N_2O}$ reported by McCabe and Wong (13) yields a value of 1.9×10^{-6}, while the straight line B on the lean side yields a value of 0.7×10^{-6}. The extremely small value of S_{N_2O} (1.9×10^{-6}) (much smaller than the value of 4×10^{-3} reported on clean Pt surfaces (16)), determined in this work for the rich reaction conditions under which the catalytic surface is predominantly covered by adsorbed CO species, appears to be consistent with the strong steric inhibition effect of the adsorbed CO species on the N_2O adsorption (17, 18). The even smaller sticking coefficient of N_2O measured from the lean conditions may be related to the self-poisoning effect of oxygen produced from the dissociation of N_2O as discussed earlier. Our

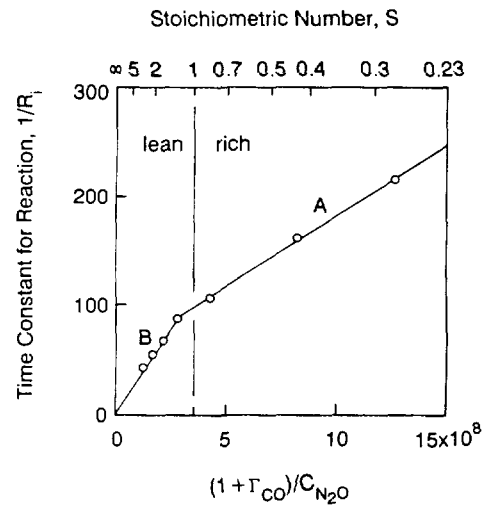

FIG. 8. Determination of adsorption sticking coefficient of N_2O (T = 583 K).

previous estimation of 2×10^{-3} for S_{N_2O} (12) based on the available literature data can be considered a reasonable upper bound for S_{N_2O} when allowing for statistical error bands (±10% to ±20%) in the published values of the activation energy of CO desorption, N_2O desorption, and N_2O dissociation. Based on the previously reported relationship between S_{N_2O} and the rate-enhancement factor (12), it can be concluded that the rate of the intermediate N_2O + CO reaction in the overall NO + CO reaction system is *at least* 2–3 orders of magnitude faster than the rate of the isolated N_2O + CO reaction.

Rate-Limiting Step of Isolated N_2O + CO Reaction

For further analysis, it is convenient to rewrite Eq. [22] as

$$\tau_r = \tau_s + \tau_a, \qquad [24]$$

by defining τ_s and τ_a as

$$\tau_s = \frac{1 + K_{CO}C_{CO}}{k_{N_2O}K_{N_2O}C_{N_2O}}, \qquad [25]$$

$$\tau_a = \frac{1 + K_{CO}C_{CO}}{k_{a,N_2O}C_{N_2O}}. \qquad [26]$$

Physically, τ_s represents the time constant for the surface reaction when the Langmuir adsorption equilibrium is established for the N_2O adsorption process, while τ_a represents the time constant for the adsorption of N_2O. The ratio of τ_a to τ_s determined from Fig. 8 yields

$$\tau_a/\tau_s = k_{N_2O}K_{N_2O}/k_{a,N_2O} \simeq 4. \qquad [27]$$

Equation [27] clearly indicates that the N_2O adsorption process is the major rate-controlling step for the isolated N_2O + CO reaction, while the surface reaction process is only the minor controlling step. More precisely, approximately 80% of the N_2O + CO reaction rate is controlled by the N_2O adsorption process, while the remaining 20% is controlled by the surface reaction rate at 583 K. In this regard, it is useful to note that the rate of N_2O adsorption increases almost linearly with the increase in the gas-phase N_2O concentration. This then suggests that the apparent reaction order of the isolated N_2O + CO reaction is expected to be somewhat less than 1.0 with respect to the N_2O concentration, in agreement with the experimental observation by McCabe and Wong (13).

DISCUSSION

Although participation of the N_2O + CO reaction as an intermediate step in the overall NO + CO reaction system has been reported previously (9, 13), its importance has not yet been well established in view of the extremely slow rate of the dissociative N_2O adsorption observed by McCabe and Wong (13). That is, the rate of the N_2O + CO reaction appeared too slow to be important as an intermediate reaction in the relatively fast NO + CO reaction system. In this work, we were able to experimentally verify the previous theoretical predictions (12) regarding the importance of N_2O formation and its subsequent reaction with CO during the NO + CO reaction over supported Rh catalysts. First, we have shown that the apparent suppression of product selectivity to N_2O formation observed at high temperatures above 300°C (9, 13) is not due to the absence of N_2O formation, but is due to the fast surface reaction of the intermediate N_2O with CO following the formation of N_2O. This means that the N_2O formation and the intermediate N_2O + CO reaction are important *at all temperature levels below 500°C* during the NO + CO reaction over Rh/Al_2O_3.

Previously, the RLS of an isolated N_2O + CO reaction was believed to be either dissociative N_2O adsorption (13) or dissociation of adsorbed N_2O (14). (Note that the *dissociative N_2O adsorption* denotes a lumped process resulting from the combination of N_2O adsorption and N_2O_a dissociation. Thus, it should not be confused with N_2O adsorption or N_2O_a dissociation.) However, this work has revealed through an extended kinetic analysis that the RLS of the isolated N_2O + CO reaction is N_2O adsorption from the gas phase to the catalytic surface. The reason behind this difference between our findings and previous findings can be traced back to the different values of the N_2O adsorption sticking coefficient employed: McCabe and Wong (13), and Belton and Schmieg (14) assumed it to be 1.0 and 0.5, respectively, whereas our detailed kinetic analysis of the steady-state N_2O + CO reaction has yielded for the first time an extremely small value for the N_2O adsorption sticking coefficient on the order of 10^{-6}.

It is noted in Figs. 1–3, and 7 that the NO conversion curve below the reaction lightoff temperature always coincides with the N_2O formation curve, in agreement with the existing literature data (9, 13). This suggests that the formation of N_2O plays an important role in sustaining the NO + CO reaction at low temperatures. This observation can be explained by the vacant surface sites being created on the surface through the desorption of N_2O_a following its formation from N_a and NO_a. Without the formation of N_2O at low temperatures, the steady-state catalytic surface would be covered predominantly by the strongest adsorbate, N_a (8). Due to the formation of N_2O, however, the strongly adsorbed nitrogen atoms are scavenged from the surface to create more vacant sites, eventually leading to the lightoff of the NO + CO reaction. More detailed kinetic analysis regarding the role of N_2O formation in the onset of the NO + CO reaction will be presented in a subsequent paper.

A series of cycling experiments between the NO + CO reaction and the N_2O + CO reaction has indicated that the surface coverage under the steady-state conditions of the NO + CO reaction is more favorable to the N_2O + CO reaction than that under the steady-state conditions of the N_2O + CO reaction. In light of the strong inhibition effect of the predominant surface species CO_a during the isolated N_2O + CO reaction (12, 13), the favorable reaction condition for the intermediate N_2O + CO reaction during the overall NO + CO reaction can be attributed to the beneficial effect of NO_a which can scavenge CO_a from the catalytic surface via both *desorptive scavenging* and *reactive scavenging*. That is, NO_a dissociates to N_a and O_a, of which N_a facilitates the desorption of CO_a from the catalytic surface due to the repulsive interaction between N_a and CO_a (12, 19) (desorptive scavenging), while O_a scavenges CO_a via CO_a–O_a reaction producing CO_2 (reactive scavenging). (Note that the desorption activation energy of CO is a function of both θ_{CO} and θ_N (12).) Combining the results of the cycling experiments with the conclusions made in the preceding paragraph regarding the beneficial effect of the N_2O formation on the onset of the NO + CO reaction, we may now say that the formation, and subsequent reaction with CO, of N_2O is not only an integral part of the NO + CO reaction, but also it interacts with the latter (i.e., NO + CO reaction), resulting in a kinetic synergism, in the sense that the overall reaction benefits from the intermediate reaction and vice versa.

Previously, N_2O formation has also been observed on both Pt/Al_2O_3 and Pt/CeO_2 during NO decomposition (15) as well as on Pt impregnated on various oxide supports during the NO + CO reaction (20). It thus appears that the formation of N_2O as an intermediate reaction product during the NO + CO reaction is an intrinsic characteristic of supported noble metal catalysts. On supported Rh catalysts, some N_2O may form via gem-dinitrosyl species ($Rh(NO)_2$) (21). However, the mechanistic importance of the N_2O formation through the gem-dinitrosyl species over noble metal catalysts is not well established, and may warrant further study.

Although this paper, along with the previous one, has focused exclusively on the N_2O intermediate during the NO + CO reaction, we believe a similar approach can be applied to other reaction systems in which the existence of a short-lived surface intermediate plays an important role in the overall reaction kinetics. Among notable examples are the molecularly adsorbed oxygen during various oxidation reactions over noble metal catalysts (22–24) and the dinitrosyl intermediate during the NO + CO reaction over Fe catalysts (25). Also, the effect of the isocyanate intermediate on the overall NO + CO reaction kinetics may be an interesting kinetic problem where this approach can be applied, even though it has been reported that the NCO species present on the Rh surface does not significantly affect the overall kinetics of the NO + CO reaction (5, 26). In any case, we believe it is essential to develop a sound kinetic model based on elementary surface processes in order to gain better insight into the given catalytic process.

SUMMARY AND CONCLUSIONS

In agreement with the theoretical prediction reported previously (12), both steady-state and transient pulse experiments conducted using fixed-bed reactors and isotopic reactants (^{13}CO and ^{15}NO) have demonstrated the mechanistic importance of the formation of N_2O and its subsequent reaction with CO during the NO + CO reaction over supported Rh catalysts. The major findings are listed below.

1. Results indicate that the two-step reaction pathway involving the formation of N_2O and its subsequent reaction with CO can make a major kinetic contribution in the NO + CO reaction system over supported Rh catalysts, independent of the support composition, over the entire temperature range of our interest (i.e., 200–500°C).
2. The reason that N_2O has generally not been observed at high temperatures above 300°C during the NO + CO reaction is not the absence of N_2O formation, but its fast reaction with CO particularly when N_2O_a reacts directly as a surface intermediate. This means that the rate of the intermediate N_2O + CO reaction is as fast as, or even faster than, the rate of the overall NO + CO reaction, confirming the theoretical predictions.
3. The onset of the NO + CO reaction is always accompanied by the formation of N_2O, suggesting that the removal of strongly adsorbed nitrogen atoms from the catalytic surface via the N_2O formation process may be a critical step for the lightoff of the NO + CO reaction over supported Rh catalysts.
4. The rate of the steady-state N_2O + CO reaction is limited primarily by the rate of N_2O adsorption. The adsorption sticking coefficient of N_2O was estimated to be extremely small—approximately 2×10^{-6}—under typical N_2O + CO reaction conditions.

It is hoped that this new understanding will help us to further expand our understanding of the mechanism of the NO + CO reaction over noble metal catalysts, eventually leading us to improve the efficiency of noble metal utilization in three-way catalytic converters.

APPENDIX A: NOMENCLATURE

a_m external surface area of a single catalyst particle, cm^2

C_b N_2O concentration in the bulk gas phase, mol/cm^3

C_j gas-phase concentration of species j, mol/cm^3

$C_{NO,f}$ NO concentration in the feed, mol/cm^3
C_s N_2O concentration over the catalyst surface, mol/cm^3
$k_{a,j}$ adsorption rate constant of species j, (cm^3/mol) s^{-1}
$k_{d,j}$ desorption rate constant of species j, s^{-1}
k_j dissociation rate constant of species j, s^{-1}
K_j ratio of adsorption to desorption rate constant of species j defined as $k_{a,j}/k_{d,j}$, cm^3/mol
k_m external mass transfer coefficient of N_2O, cm/s
N_p total number of catalyst particles in the reactor
Q total feed flow rate, cm^3/s
r_2 dimensionless N_2O dissociation rate constant defined as $k_{N_2O}/k_{d,CO}$ (12)
R_i rate of the isolated N_2O + CO reaction, s^{-1}
$\tilde{R}_i$ rate of the isolated N_2O + CO reaction at the transition point from the NO + CO half-cycle to the N_2O + CO half-cycle during the cyclic operation, s^{-1}
R_{max} maximum rate of N_2O formation, mol/s
R_{N_2O} rate of N_2O formation, mol/s
r_p radius of a catalyst particle, cm
S stoichiometric number defined as C_{N_2O}/C_{CO}
S_{N_2O} sticking coefficient of adsorption for N_2O under reaction conditions

Greek Letters

β dimensionless desorption rate constant of N_2O defined as $k_{d,N_2O}/k_{d,CO}$ (12)
Γ_{CO} dimensionless gas-phase concentration of CO defined as $K_{CO}C_{CO}$ (12)
Γ_{N_2O} dimensionless gas-phase concentration of N_2O defined as $\beta K_{N_2O}C_{N_2O}$ (12)
Δ inhibition function defined by Eq. [14]
η steady-state rate-enhancement factor of the intermediate N_2O + CO reaction relative to the rate of the isolated N_2O + CO reaction
$\tilde{\eta}$ transient rate-enhancement factor at the transition point of the cyclic operation, relative to the steady-state rate of the isolated N_2O + CO reaction, defined by Eq. [19]
θ_j surface coverage of adsorbed species j
τ_a time constant for N_2O adsorption in N_2O + CO system defined by Eq. [26], s
τ_o overall time constant for N_2O + CO reaction defined by Eq. [21], s
τ_r time constant for N_2O + CO reaction near the stoichiometric condition defined by Eq. [22], s
τ_s time constant for N_2O + CO reaction on the surface under Langmuir adsorption equilibrium condition defined by Eq. [25], s
τ_∞ time constant for N_2O + CO reaction under extremely lean conditions defined by Eq. [23], s

Subscripts

a adsorbed state
i isolated N_2O + CO reaction system
j chemical species (j = NO, CO, N_2O, or N)
o overall NO + CO reaction system
v vacant surface sites

APPENDIX B: EFFECT OF EXTERNAL MASS TRANSFER RESISTANCE ON THE OBSERVABILITY OF N_2O FORMATION

For a single catalyst particle under steady-state reaction conditions, the rate of N_2O formation (R_{N_2O}) must be equal to the mass transfer rate of N_2O from the catalyst surface to the bulk gas stream if the intermediate N_2O + CO reaction is absent. That is,

$$a_m k_m (C_s - C_b) = R_{N_2O}. \quad [B1]$$

Assuming complete conversion of NO to N_2O, we can estimate the maximum rate of N_2O formation (R_{max}) over a single particle by

$$R_{max} = 0.5 Q C_{NO,f}/N_p. \quad [B2]$$

Combining Eqs. [B1] and [B2] yields

$$\frac{C_s}{C_b} - 1 \le \frac{R_{max}}{a_m k_m C_b}. \quad [B3]$$

For the experimental conditions used for Fig. 1,

$R_{max} = 6.275 \times 10^{-13}$ mol/s,
$a_m = 4\pi r_p^2 = 7.069 \times 10^{-4}$ cm^2,
$k_m = 2.8 \times 10^2$ cm/s (at 600 K),
$C_b = 5.625 \times 10^{-9}$ mol/cm^3 (at the N_2O peak of 126 ppm),

where the average particle diameter was taken to be 150 μm, and k_m was calculated using the mass transfer correlation derived by analogy from the Ranz–Marshall equation for heat transfer (27). With these numerical values, Eq. [B3] yields

$$\frac{C_s}{C_b} - 1 \le 4.42 \times 10^{-3}. \quad [B4]$$

Equation [B4] indicates that the N_2O concentration in the bulk gas phase is essentially the same as that over the catalyst surface. This means that, under the given experimental conditions, the effect of the external mass transfer

resistance is negligible on the observability of N_2O formation during the overall NO + CO reaction. Thus, the absence of N_2O in the bulk gas phase at high temperatures (e.g., at 325°C) shown in Fig. 1 cannot be attributed to the external mass transfer limitations.

REFERENCES

1. Campbell, C. T., and White, J. M., *Appl. Surf. Sci.* **1,** 347 (1978).
2. Dubois, L. H., Hansma, P. K., and Somorjai, G. A., *J. Catal.* **65,** 318 (1980).
3. Taylor, K. C., and Schlatter, J. C., *J. Catal.* **63,** 53 (1980).
4. Hecker, W. C., and Bell, A. T., *J. Catal.* **84,** 200 (1983).
5. Hecker, W. C., and Bell, A. T., *J. Catal.* **85,** 389 (1984).
6. Taylor, K. C., *in* "Catalysis: Science and Technology" (J. R. Anderson and M. Boudart, Eds.), Vol. 5. Springer-Verlag, Berlin, 1984.
7. Root, T. W., Schmidt, L. D., and Fisher, G. B., *Surf. Sci.* **134,** 30 (1983).
8. Oh, S. H., Fisher, G. B., Carpenter, J. E., and Goodman, D. W., *J. Catal.* **100,** 360 (1986).
9. Cho, B. K., Shanks, B. H., and Bailey, J. E., *J. Catal.* **115,** 486 (1989).
10. Oh, S. H., *J. Catal.* **124,** 477 (1990).
11. Cho, B. K., *J. Catal.* **131,** 74 (1991).
12. Cho, B. K., *J. Catal.* **138,** 255 (1992).
13. McCabe, R. W., and Wong, C., *J. Catal.* **121,** 422 (1990)
14. Belton, D. N., and Schmieg, S. J., *J. Catal.* **138,** 70 (1992).
15. Cho, B. K., and Stock, C. J., *in* "1986 Annual Meeting of American Institute of Chemical Engineers, Miami Beach, FL, Nov. 1986."
16. Weinberg, W. H., *J. Catal.* **28,** 459 (1973).
17. Shi, S.-K., and White, J. M., *J. Chem. Phys.* **73,** 5889 (1980).
18. Daniel, W. M., Kim, Y., Peebles, H. C., and White, J. M., *Surf. Sci.* **111,** 189 (1981).
19. Root, T. W., Schmidt, L. D., and Fisher, G. B., *Surf. Sci.* **150,** 173 (1985).
20. Kudo, A., Steinberg, M., Bard, A. J., Campion, A., Fox, M. A., Mallouk, T. E., Webber, S. E., and White, J. M., *J. Catal.* **125,** 565 (1991).
21. Hyde, E. A., Rudham, R., and Rochester, C. H., *J. Chem. Soc., Faraday Trans I* **80,** 531 (1984).
22. Yates, J. T., Jr., Thiel, P. A., and Weinberg, W. H., *Surf. Sci.* **82,** 45 (1979).
23. Fisher, G. B., Sexton, B. A., and Gland, J. L., *J. Vac. Sci. Technol.* **17,** 144 (1980).
24. Monroe, D. R., and Merrill, R. P., *J. Catal.* **65,** 461 (1980).
25. Casewit, C. J., and Rappe, A. K., *J. Catal.* **89,** 250 (1984).
26. Solimosi, F., and Sarkany, J., *Appl. Surf. Sci.* **3,** 68 (1979).
27. Bird, R. B., Stewart, W. E., and Lightfoot, E. N., "Transport Phenomena," Wiley, New York, 1960.